Research Article

Chemical Review and Letters

journal homepage: www.chemrevlett.com

ISSN (online): 2645-4947 (print) 2676-7279

Obtaining an organic-inorganic sorbent based on vermiculite modified with urotropine and hydrolyzed polyacrylonitrile

Sabokhat Kholmurodova[1], *, Khayit Turaev[1], Rustam Alikulov[1], Khasan Beknazarov[2], Abror Nomozov[3,4], Khurshid Eshmurodov[5]

[1]*Department of Chemistry Termez State University, Termez, P. O. Box: 19100, Uzbekistan.*
[2]*Department of General Medicine, Angren University. Tashkent, Uzbekistan.*
[3]*Department of Chemical Engineering, Termez State University of Engineering and Agrptechnologies. Termez, P. O. Box: 19100, Uzbekistan.*
[4]*Department of Medical and Biological Chemistry, Termez Branch of Tashkent Medical Academy. Termez, P. O. Box: 19100, Uzbekistan.*
[5]*Department of Inoorganic Chemistry, Tashkent Institute of Chemical Technology, Tashkent, Uzbekistan.*

ARTICLE INFO

Article history:
Received 30 September 2024
Received in revised form 04 February 2025
Accepted 16 February 2025
Available online 16 February 2025

Keywords:
Vermiculite
Hydrolyzed polyacrylonitrile
Porosification
Urotropin
Hydrolyzed Polyacrylonitrile

ABSTRACT

In this article presents information about the modification of vermiculite with hydrolyzed polyacrylonitrile and the synthesis of organic-inorganic sorbent obtained by adding hexamine as a surface-active group. Morphological images of the composite material obtained based on SEM analysis show the changes. below, surface area sizes were calculated based on isotherms drawn based on the results of adsorption-desorption using water vapor. The static and dynamic exchange capacities of the sorbent were studied. It was determined that the highest SAS value was 13 mmol-eq/g and DAS value was 1 mmol-eq/g in the presence of Cu2+ ion solution. The thermal tolerance of the obtained sorbent, SEM images of the surface, elemental analysis and the structure of existing bonds were analyzed using novel-infrared spectroscopy methods. Based on the BET method by absorbing water vapor at low pressure, the studied structural sorption properties of the sorbent showed that they have a mesoporous structure and high sorption properties.

1. Introduction

In the areas where there is industrial production, the high level of wastewater pollution with heavy metals pollutes the soil [1]. Most of the clay minerals retain these metals due to their natural sorbent properties [2,3]. Changing vermiculite with various metals and orga[nic substances allows it to absorb ions [4]. Experimental evidence shows that vermiculite saturated with Mg, Cu, Na adsorbs ammonia mainly as ammonium ion [2]. Manganese oxide-modified vermiculite was prepared as an adsorbent for the separation of Rhodamine B dye from aqueous solution, and morphological analysis showed that the addition of manganese oxide to vermiculite created a porous surface that facilitated the separation of RhB from aqueous solution [4]. Radioactive cesium ($137Cs^+$) is one of the most dangerous decay products in radioactive liquid waste due to its large inventory, long half-life (t 1/2 ~ 30 years) and high environmental mobility [5-7]. Vermiculite was used to absorb malachite green, a substance used in paints. To increase the adsorption potential of vermiculite, Cu was reinforced with a metal-organic framework [8]. A composite adsorbent consisting of $BaCl_2$ embedded in expanded vermiculite was synthesized and tested in a laboratory-scale adsorption device [9]. A vermiculite/graphene and polyacrylamide composite has been proposed as an effective adsorbent for the removal of Congo red dye pollution in aquatic ecosystems [10,11]. Cooling chemisorption adsorption systems on vermiculite matrix composite sorbents have been found to be advantageous due to the large change in concentration compared to physisorption [12]. The main property of vermiculite is that it can withstand salt swelling during the reaction between ammonia and salt [13]. Expanded vermiculite-based "salt in porous matrix" composites have excellent methanol sorption and heat storage capabilities [12,13]. In the research on the adsorption of radioactive cesium $137Cs^+$, it was found that various clay minerals from the critical zone of the earth have great potential for cleaning

---

* Corresponding author e-mail: abrornomozov055@gamil.com
https://doi.org/10.22034/CRL.2025.481061.1435

metal ions [14]. It was confirmed that Cs ions replaced Mg ions in the crystal [6,7]. The effect of $137Cs^+$ adsorption on the structure of vermiculite clay minerals in suspensions was determined [14,15]. The degree of sorption of activated vermiculite to Mn^{2+} is higher than to Ni^{2+}, Cu^{2+}. The sorption results show that the formation of an amorphous phase [16] improved the sorption capacity characteristics when treating vermiculite with Na_2HPO_4*12H2O. For As, Ba, Cd, Co, Cr, Cu, Mn, Ni, Pb, Sr, suitability of vermiculite and K10 montmorillonite for separation and pre-concentration of elements was studied [16,17]. Aimed at a comprehensive evaluation of the hydration kinetics of magnesium chloride and potassium carbonate embedded in the vermiculite host matrix for thermochemical energy storage applications [18]. Sorption heat storage is a promising technology aimed at efficient use of renewable energy sources [19]. Materials based on hygroscopic salts and their hydrates have a high potential for heat storage [20]. The level of porosity of composite materials is studied on the basis of morphological analysis and tests carried out to determine the surface [21]. Calculations based on these indicators provide information about the properties of the substance on the surface [22-25].

The aim of this study was to obtain an organo-inorganic sorbent by modifying the natural sorbent clay mineral vermiculite with organic substances containing amino groups (hydrolyzed polyacrylonitrile, urotropine).

2. Materials and Methods

2.1. Materials

The following chemicals were used for the research: vermiculite, maleic anhydride, hydrolyzed polyacrylonitrile, hexamethylene, tetraamine, hydrochloric acid, ammonia water, distilled water.

2.2. Methods

2.2.1. IR analysis

The composition of the sorbent was investigated using IR-spectrium analysis with Shimadzu IR Tracer-100(SHIMADZU (Japan).

2.2.2. SEM-EDX- analysis

The images of the surface of the sorbent obtained in different sizes were taken on a JSM-IT200 device with elemental dispersion analysis (SEM - EDX) belonging to the Japanese company JEOL.

2.2.3. TGA and DTA analysis

Olingan sorbentlarning fizik-kimyoviy xossalarini harorat ta’siridagi o’zgarishlarni termogravimetrik tadqiqotlar DTG-60, SHIMADZU qurilmasida (Yaponiya) o‘rganildi.Tahlil sharoiti: Argon muhiti(80mi/min)da, harorat oshib borishi tezligi-10C/daqiqada olib borildi.

2.2.4. Mak-Ben-Bakra analysis

Thermogravimetric studies of changes in the physicochemical properties of the obtained sorbents under the influence of temperature were studied on the DTG-60 device, SHIMADZU (Japan). Analytical conditions: in an argon atmosphere (80 mi/min), the rate of temperature increase was -10C/min.

2.2.5. Synthesis of sorbent

For research, vermiculite was expanded, activated, and modified with hydrolyzed polyacrylonitrile and hexamine. Vermiculite crushed and passed through a 0.5 mm sieve was placed in a sintering furnace at a temperature of 700 ºC for expansion. (Korea DaiHan FHX-05 Programmable Digital Muffle Furnace (4.5L)). Expansion causes the density of vermiculite to decrease many times as a result of the release of chemically bound water between the vermiculite layers. In order to increase the surface area of vermiculite, it was treated with 15% hydrochloric acid solution. In order to remove acid residues, it was neutralized with soda water and decanted. It was built in a drying oven for 36 hours at a temperature of 100-105 ºC. Hydrolyzed polyacrylonitrile (GIPAN) was impregnated into vermiculite by in-situ method. GIPAN binds with vermiculite layers with –OH+ bonds and forms a composition. The composite was modified by adding hexamine with surface-active functional groups. The polymer-composite mass was poured into a ceramic crucible and dried by directing air flow. The fully dried sample was divided into small pieces. The obtained substance is porous, activated vermiculite: hydrolyzed polyacrylonitrile: hexamine (EAV-HPG) is a brown-yellow, porous, hard and resinous mass. In the copolymerization reaction, when vermiculite: GIPAN: hexamine substances were obtained in mass ratios of 2:4:0.5, the reaction yield was equal to the highest indicator (97%).

2.2.6. Study of the static exchange capacity of the obtained sorbent

Sorption of the obtained sorbent in a solution containing metal ions was studied. For this, 250 ml of 0.1 N metal sulfate, chloride and nitrate solutions (pH = 4.2) were prepared. In order to determine the static exchange capacity (SEC) of the sorbent: glass ampoules were filled with 10 ml of the prepared solution and 0.03 g of ion exchanger. Ampoules are left for 24 hours. Researches were conducted at temperatures of 293 K, 303 K, 313 K, the optimal polycondensation temperature was found to be 303 K. The composition of the initial i.e., standard solution of copper (II) ions and the concentration of the solution containing the sorbent were determined using an ultraviolet spectrophotometer of the solution (SHIMADZU, Japan). In this case, the ammonia complex of the copper ion solution was prepared and its concentration was determined by measuring the optical density [26,27].

To determine the concentration, the concentration of the standard solution containing metal ions, that is, the concentration of the solution without the initial sorbent and the concentration of the solution with the ion exchange sorbent, is found by multiplying the solution volume by the ratio of the dry sorbent mass. Zn 2+ available solution concentrations were determined by complexometric titration. Based on the results obtained by ultraviolet spectrophotometric and potentiometric titration, the number of metal ions absorbed in the EAV-HPG sorbent and the sorption capacity were calculated according to the Eq. 1:

$$q_e = \frac{(C_0 - C_M)\cdot V}{m} \quad (1)$$

here:

q_e-sorption capacity of the ion exchanger, mmol/g;

C_0-the concentration of the ion-exchanged undiluted solution in mmol/l;

CM - equilibrium concentration (concentration of solution containing ion exchange sorbent, mmol/l;

V – solution volume, l;

m - mass of dry sorbent, g.

Scheme 1 shows the proposed formulation of a sorbent based on vermiculite modified with hexamethylenetetramine and hydrolyzed polyacrylonitrile. Nitrogen in the amide group of hydrolyzed polyacrylonitrile is connected to the carbon atom of hexamethylenetetramine. Hydroxyl groups on the surface of vermiculite silicate layers are oxidized using maleic anhydride and connected to another carbon atom in the main chain of hexamethylenetetramine. In the process of modification of silicate layers, the presence of other links of the hydrolyzed polymer, and the possibility that maleic anhydride and hydrolyzed polyacrylonitrile have contaminated other functional groups are also not excluded.

2.3. Study of the dynamic exchange capacity of the obtained sorbent.

The dynamic exchange capacity (DEC) method of the sorbent is based on the absorption of ions from the solution flowing at a certain speed through the column in which the pieces of the sorbent in the granule state are placed [28,29]. The sorbent particles were placed in a column with a diameter of 10 mm and a length of 20 cm, and 0.5;1; A solution containing a metal ion was passed slowly at speeds of 2 ml/min, and the results are presented in Table 1.

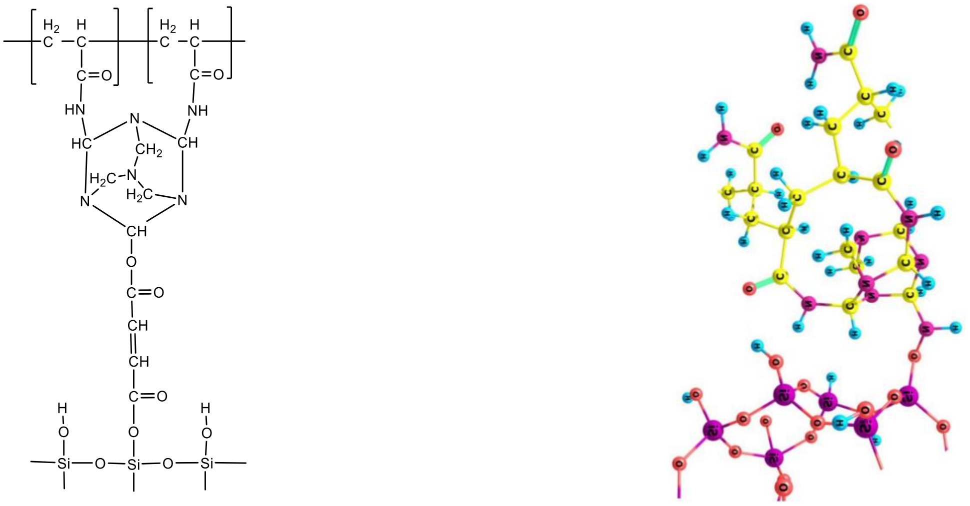

a) b)

Scheme 1. Vermiculite-based sorbent modified with hexamethylenetetramine and hydrolyzed vermiculite. a) molecular formula b) spherical stergen model

Table 1. Composition of initial substances of EAV-HPU sorbent and characteristics of ion exchange.

Vermiculite, GIPAN and	Reaction yield, %	Static exchange capacity in 0.1 N solution, mg-eq/g		Dynamic exchange capacity in 0.1 N solution, g/dm^3					
		$CuSO_4$	$ZnSO_4$	$CuSO_4$			$ZnSO_4$		
				0.5ml/min	1ml/min	2ml/min	0.5ml/min	1ml/min	2ml/min
4:2:05	58%	5.1	4.1	0.503	0,408	0.205	0.402	0,304	0.200
1:1:0.5	75%	6.1	3.5	0.605	0,494	0.150	0.385	0,302	0.202
2:4:0.5	95%	9.5	6.1	0.625	0,405	0.205	0.450	0,305	0.205

2.4. IR- analysis

2.4.1. IR- analysis of the hydrolyzed polyacrylonitrile

When synthesizing these sorbents, the IR spectra of the starting materials were also analyzed. In the IR spectroscopy spectrum of hydrolyzed polyacrylonitrile obtained for the modification of vermiculite, valence and deformation vibrations belonging to the OH group were formed in the region of 3266.40 cm-1 and 1176.58 cm-1. Intensive valence and deformation peaks of the N-H group appeared at vibration frequencies of 3223.05 cm-1 and 1603.63 cm-1. Moderately intensive valence and deformation peaks of the C-H group appeared at 2822.1 cm-1, 1047.35 cm^{-1} and 769.60 cm-1. The vibration frequency of the C=O bond was observed in the region of 1633.86 cm-1, and the valence vibrations of the COO- groups were observed in the region of 1514.12 cm^{-1} (Figure 1).

2.4.2. IR- analysis of the urotropin

In the analysis of the IR spectra of the urotropin sample, moderately intense peaks in the regions of 2985.81 cm-1 and 2885.51 cm-1 were formed, which belonged to C-H, and a strong absorption frequency of the C-N bond at a vibration frequency of 958.62 cm-1 (Figure 2).

2.4.3. IR- analysis of the Maleic anhydride

The valence and deformation vibration frequencies of C-H bonds were observed in the regions of 2922.16 cm-1, 2852.12 cm-1, 1456.26 cm-1, 731.02 cm-1. Medium-intensity peaks of lactans were observed in the regions of 1869.02 cm-1, 1828.52 cm-1 and 1770.65 cm-1, and strong-intensity symmetric vibration frequencies of C=O bonds were observed in the regions of 1716.65 cm-1, as well as an absorption peak of C-O-C group in the region of 1269.16 cm^{-1} (Figure 3).

2.4.4. IR spectrum analysis of the EAV-HPG sorbent

The IR spectra of the EAV-HPG sorbent obtained based on urotropin and hydrolyzed polyacrylonitrile were studied and analyzed, and the results obtained are presented in Figure 4 and Table 2.

Expanded vermiculite was activated in strong acids (15% H2SO4 and 7% HCl) to increase the surface area (Figure 5). It was found that the sorption level of activated vermiculite reached 2 mg-eq/g.

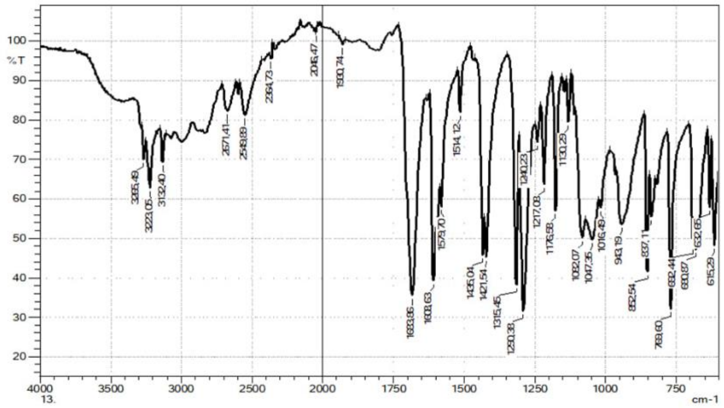

Fig. 1. IR-spectroscopy spectrum of hydrolyzed polyacrylonitrile

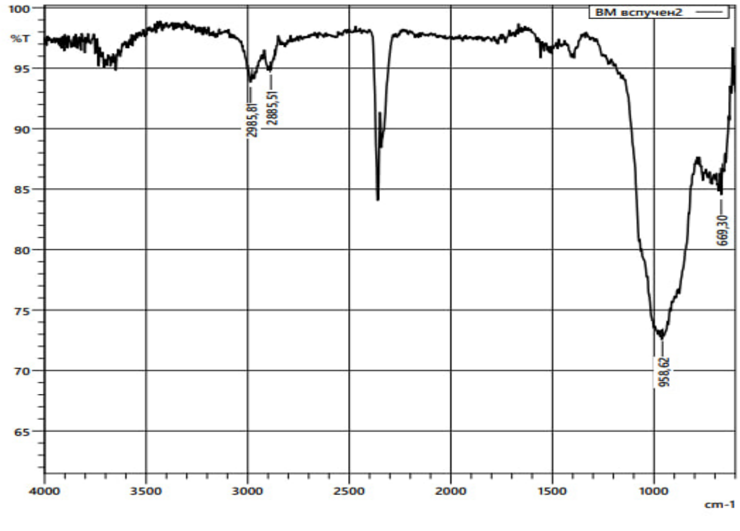

Fig. 2. IR spectrum of the urotropin

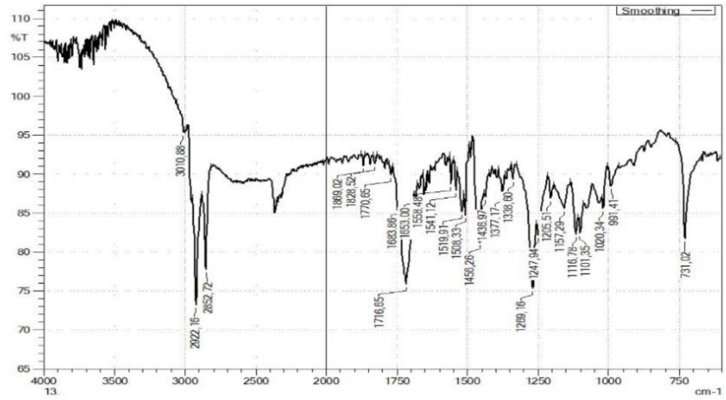

Fig. 3. IR spectrum of the maleic anhydride

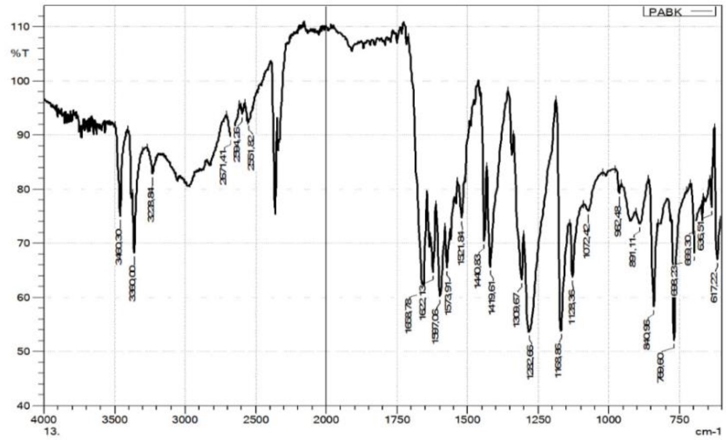

Fig. 4. IR spectrum analysis of the obtained EAV-HPG sorbent

Table 2. IR spectrum analysis results of EAV-HPG sorbent

Functional groups	**Vibration type**	**Absorption area (-cm)**	**Functional groups**	**Vibration type**	**Absorption area (-cm)**
OH	valence	3460,30	C=O	valence	1622,13
NH_2	valence	3360,00	OH	deformation	1597,91
NH	valence	3228,84	N-H(NH_2)	deformation	1573,91
C-H	valence	2882,1	N-H(NH)	deformation	1521,84
N-H	valence	2671,41	C-H	deformation	1440,83
Si-H	symmetrical	21,82	C-O-C	deformation	1282,66
C-H	deformation	769,60	Si-O	valence	1128,36

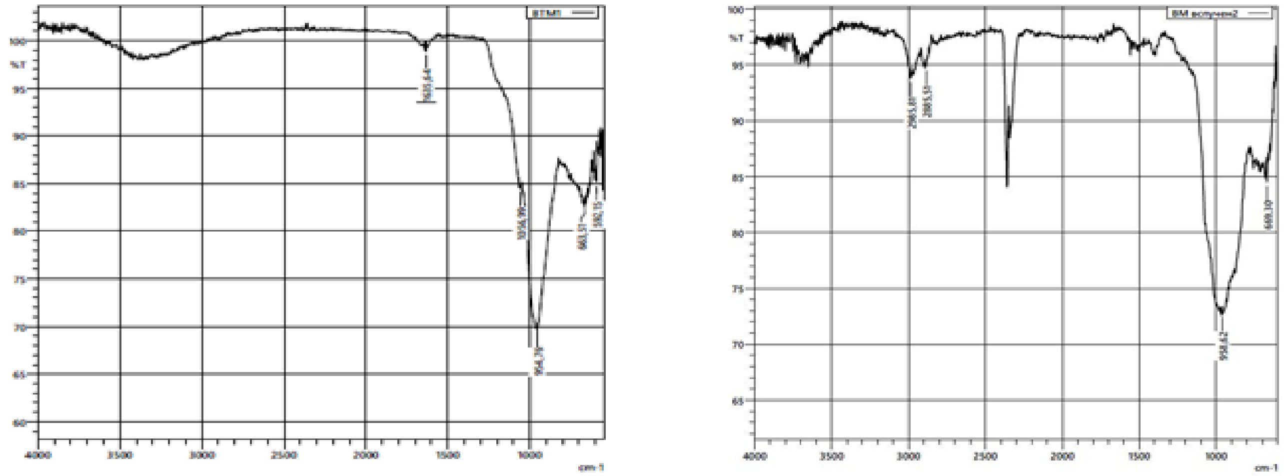

a) b)

Fig. 5. IR spectra of vermiculite from the Tebinbulak deposit, in its natural (a) and porous (b) state

2.5. TGA and DTA analysis

Differential-thermal and thermogravimetric analyzes of the thermal stability of the sorbent obtained by organic modification with hexamine and GIPAN were obtained (SHIMADZU-DTG-60 of Japan). For analysis, 4,390 mg of substance (in powder form) was taken in a porcelain crucible. Analytical process at a speed of 10 degrees/min at a temperature of up to 800 °C, T-800, TG-200, DTA - 1/10 galvanometer sensitivity, in an argon environment (gas flow of 80 ml/min) method of automatic recording of the derivatogram determined with in Figure 6.

2.6. Differential thermal analysis of the sorbent

In the differential thermal analysis of the obtained substance, one characteristic exothermic heat release was observed [29-32]. The heat release was observed at 36.65 minutes of the analysis, when the temperature reached 405.79 ºC, and ended at 48.67 minutes, when the temperature reached 494.26 ºC. The peak of heat absorption occurred at 42.27 minutes of the analysis, when the temperature reached 432.24ºC. As a result of the exothermic effect, 1.71 J (389.56J/g), i.e., 408.55mcal (93.06 cal/g) of heat was released. This leads to the conclusion that the release of heat was caused by the decomposition of the organic part of the sample in Table 3.

2.7. Thermogravimetric analysis of the sorbent sample

In the TGA analysis of the sample of the obtained substance, the decomposition of the substance under the influence of temperature took place in three stages:

-the first stage of heating started in 0.03 minutes, when the temperature reached 21.82ºC, and ended in 25.68 minutes, when the temperature reached 267.76ºC. At this stage, 0.986 mg, i.e., 22.460% of the mass of the substance was lost. The mass lost in the mentioned temperature range is due to the outflow of hygroscopic water contained in this substance and a small amount due to the decomposition of the organic part. -the second stage intensive mass loss begins when the temperature reaches 267.76 C and ends when it reaches 497.59 C. This process started at 25.68 minutes of warm-up and ended at 49.01 minutes. In mass loss, 27.768% of the mass of the sample, i.e., 1.219mg of substance, was decomposed. -the third stage the loss of the sample mass of the third stage started at 49.01 minutes of heating and lasted until 80.52 minutes. This process started when the temperature reached 497.57°C and continued up to 800°C. During this decomposition, 0.857mg of substance, i.e., 19.522% of the sample mass, was decomposed. At this stage, during the temperature rise to 303º C, the organic substances in the sample were completely decomposed [33-35].

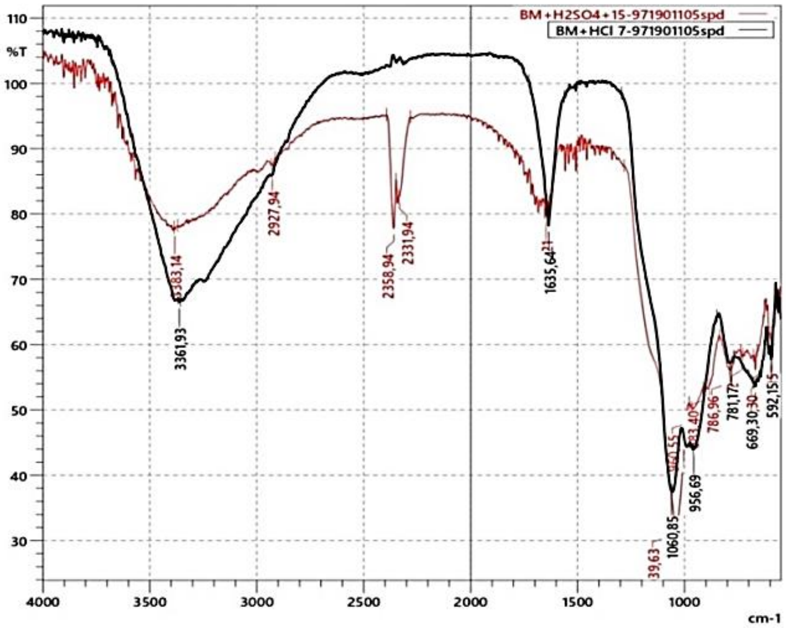

Fig. 6. IR spectroscopy analysis of vermiculite activated with 15% sulfuric acid (red lines) and 7% hydrochloric acid (black lines)

Table 3. Thermogravimetry (TGA) curve analysis of EAV-HPG composite sorbent

Mass loss stages (№)	Temperature of onset of mass loss (ºC; K)	Completion temperature of mass loss (ºC; K).	Time to onset of mass loss (min.)	Mass loss completion time (min)	Mass lost (mg)	Mass lost (%)
1	21.82, 294,82	267.76ºC, 540,76	0.03	25.68	0.986	22.46
2	267.76ºC, 540,76	497.59	25.68	49,01	1,219	27,768
3	497.59, 770,59	800	49,01	80.52	0.857	19,522

3. Results and Discussion

3.1. SEM and EDX analysis

Surface morphological images of the obtained substance were obtained. Also, in the analysis of the elemental analysis, the atoms of the sorbent sample were excited with the help of SEM-EDA electron beams, and the X-ray radiation characteristic of each element present in the sample was recorded. Using a scanning electron microscope (SEM) (Figure 7) and elemental analysis, surface images of the vermiculite composite modified with hexamethyltetraamine and hydrolyzed polyacrylonitrile at 5 µm, 10 µm, 50 µm and 200 µm sizes were obtained (Figure 7-9). The percentages of the elements in the obtained substance are shown in Table 4.

a) 5µm b) 10µm of EAV-HPG composite sorbent; c) 50 µm and d) 200 µm magnified images can be observed by analyzing the following cases [36-38]: in the 5 µm size image of the image, the whole surface of the polymer composite is shown in a smooth and homogeneous state. This image does not show traces of foreign matter. In the image of the surface of the sample taken at the size of 10 µm of the electron microscope, the micropores of the sorbent are located in a layered view on the porous bulge. The images of distribution of the elements present in the obtained sorbent are represented by the appropriate colors on the surface of the sample (Figure 9,10).

3.2. EDS elemental analysis of sorbent

From the X-ray diffractograms of the sorbent samples, we can see that the peak of the X-ray spectrum started at 2θ = 0.45° and the end of the spectrum was 2θ = 0.601°. This spectrum is the peak with the highest index, it is °2th =0.5°; It is seen that it belongs to element O. This indicator was observed due to metal oxides in vermiculite, -OH- group content and O content in GIPAN. Compiled on the basis of elemental analysis of the sample, shows that oxygen is 46.02±0.04% of the tested sample mass. After oxygen, the largest amount of mass and atomic percentage belonged to the element C. Its mass percentage was 32.16±0.02. This mass was observed due to C in organic reagents - GIPAN and urotropin. The third element with the highest mass percentage in the table is N, which is 2.37±0.02%. The percentage of nitrogen element can be seen due to amino groups and cyan group in polyacrylonitrile and geksamin Table 4.

3.3. EDX- analysis

According to the analysis results, the elements in the material range from Al-U in the EAV-HPU sample before the metal ions were added to the solution (Figure 11). Fe 5.499% (0.018 keV), K 3.544% (0.041 keV), Si 2.103% (0.064 keV), Al 0.975% (0.069 keV), and in the EAV-HPU+Cu sample after the metal ions were added to the solution (Figure 12,13).

Cu 59.986% (0.188 keV), Si 17.435% (0.726 keV), Al 6.557% (0.723 keV), Fe 5.102% (0.032 keV), K 4.768% (0.092 keV), Cl 4.748% (0.177 keV), Ti 0.969% (0.041 keV), and the elements in the material range from Na-U, in the EAV-HPU+Cu sample after the metal ions are added to the solution (Figure 14).

SiO_2 47.271% (2.649 keV), CuO 42.057% (0.076 keV), Fe_2O_3 4.887% (0.027 keV), K_2O 3.670% (0.094 keV), TiO_2 1.091% (0.027 keV), SO_3 0.816% (0.252 keV), NiO 0.090% (0.006 keV), V_2O_5 0.089% (0.014 keV), MnO 0.030% (0.005 keV), elemental results were determined in a 10 mm collimator, using the detail and powder_oxide group methods. In this method, the total mass of the analyzed substance is calculated as100%, excluding the amount of light elements.

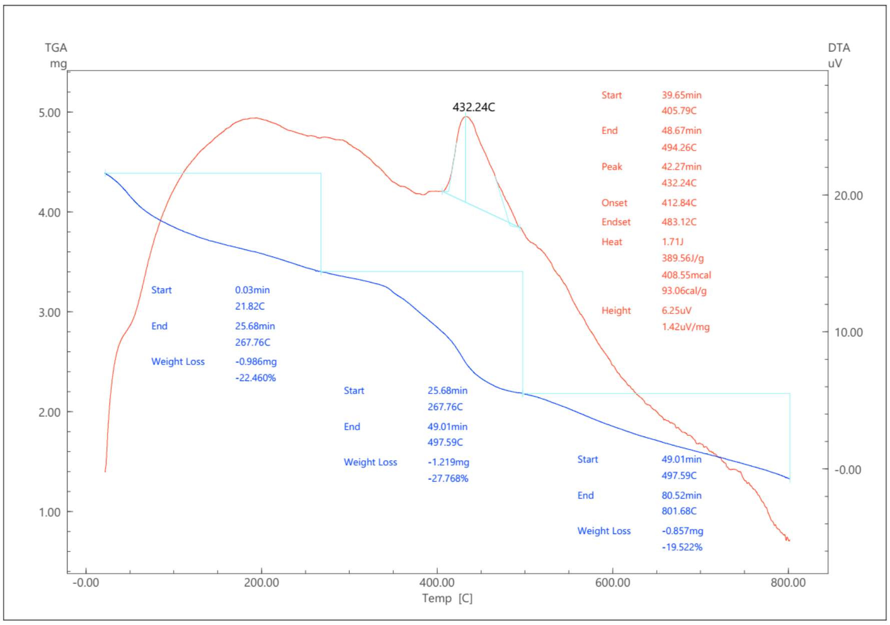

Fig 7. (DTA) and (TGA) analysis of EAV-HPG sorbent.

Table 4. Chemical composition of vermiculite from Tebinbulok mine, Republic of Uzbekistan.

Oxides	SiO_2	MgO	Al_2O_3	Fe_2O_3	CaO	K_2O	Na_2O	TiO_2	SO_3	LOI (loss on ignition (1000°C) g	Hydrogen value (ISO 787-9)pH
Amount (in %)	41,10	16,73	12,64	9,92	6,73	2,92	1,83	1,09	0,24	6,96	6,8-7,0

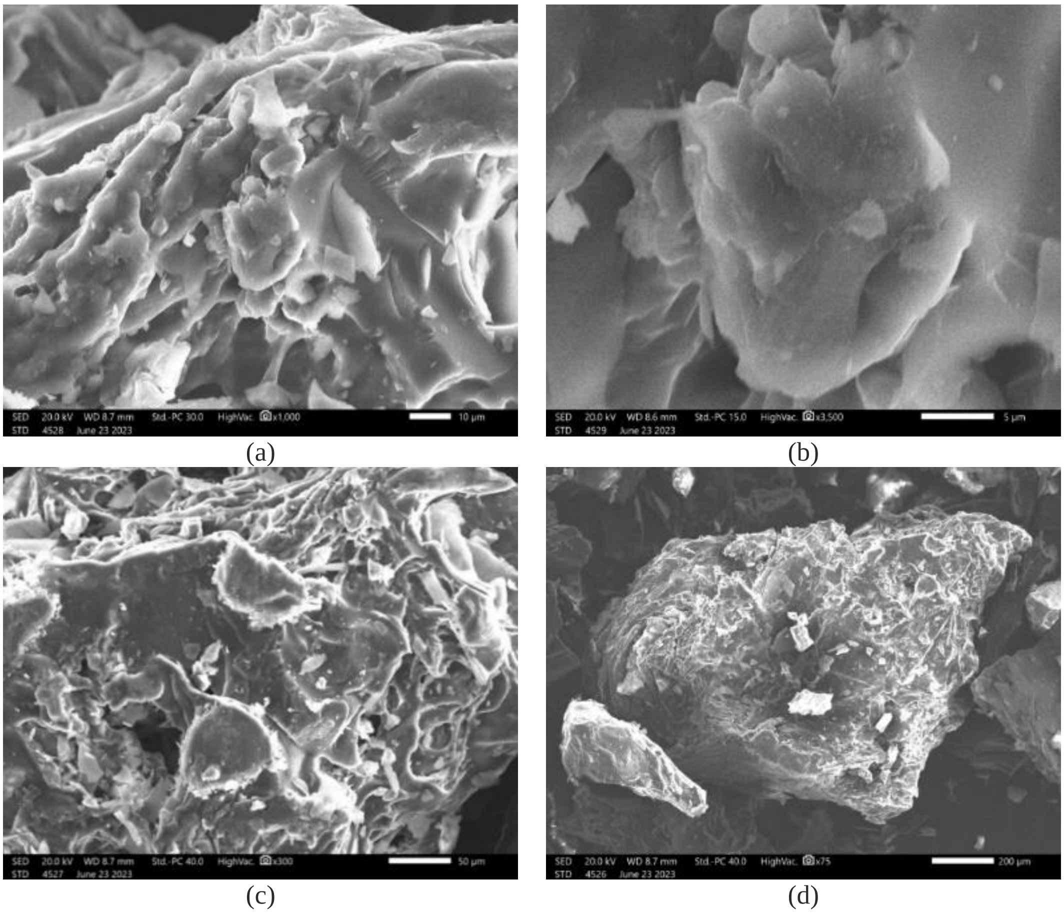

Fig 8. SEM images of the surface of EAV-HPG sorbent: a) 5μm b) 10μm; c) 50μm and d) 200μm size images state (a) and C; N; According to the elements of O (b).

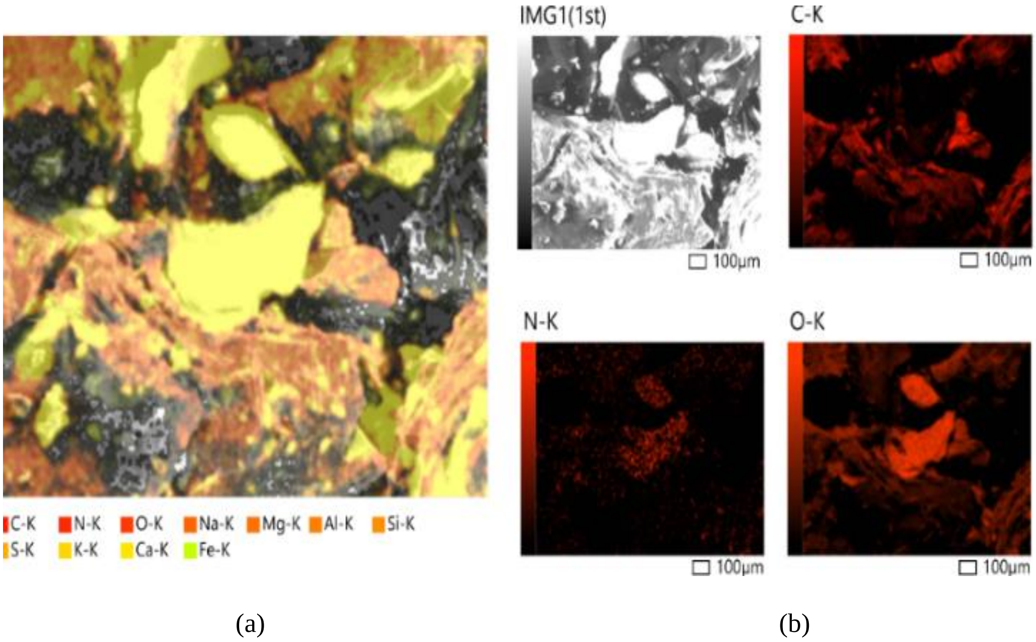

Fig. 9. Color-differentiated images of the elements contained in the EAV-HPU sorbent in the 100 μm analysis: in the general

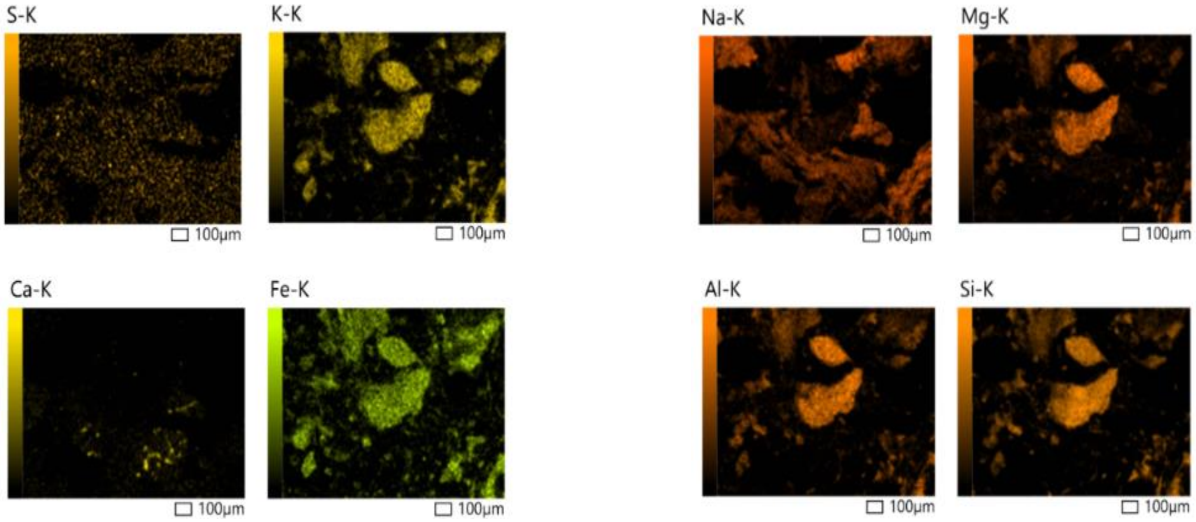

(a) (b)

Fig. 10. Color-differentiated images of elements contained in EAV-HPG sorbent in 100 µm analysis: S;K; Ca; Fe (a) and Na; Mg; Al; According to Si elements (b).

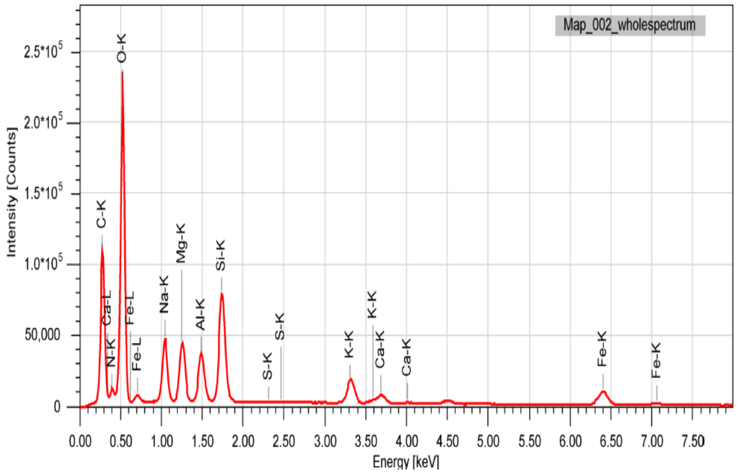

Element	Line	Mass%	Atom%
C	K	32.16±0.02	41.84±0.03
N	K	2.37±0.02	2.64±0.02
O	K	46.02±0.04	44.94±0.04
Na	K	4.50±0.01	3.06±0.01
Mg	K	3.03±0.01	1.94±0.00
Al	K	2.20±0.01	1.27±0.00
Si	K	4.68±0.01	2.61±0.00
S	K	0.04±0.00	0.02±0.00
K	K	1.74±0.01	0.70±0.00
Ca	K	0.65±0.00	0.25±0.00
Fe	K	2.62±0.01	0.73±0.00
Total		100.00	100.00

Fig. 11. Energy dispersive spectroscopy (EDS) analysis of elements in the sorbent

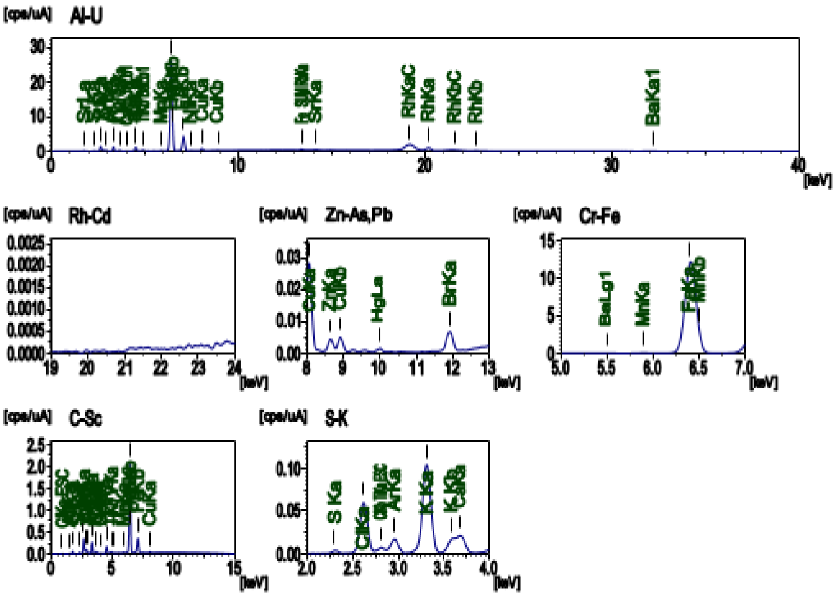

Fig. 12. EAV-HPU sample before the metal ions were added to the solution.

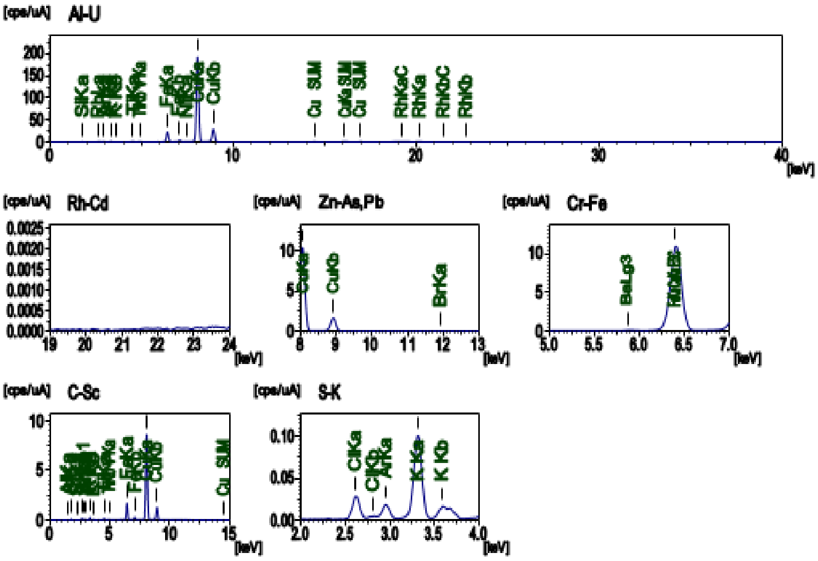

Fig. 13. EAV-HPU+Cu sample after the metal ions were added to the solution

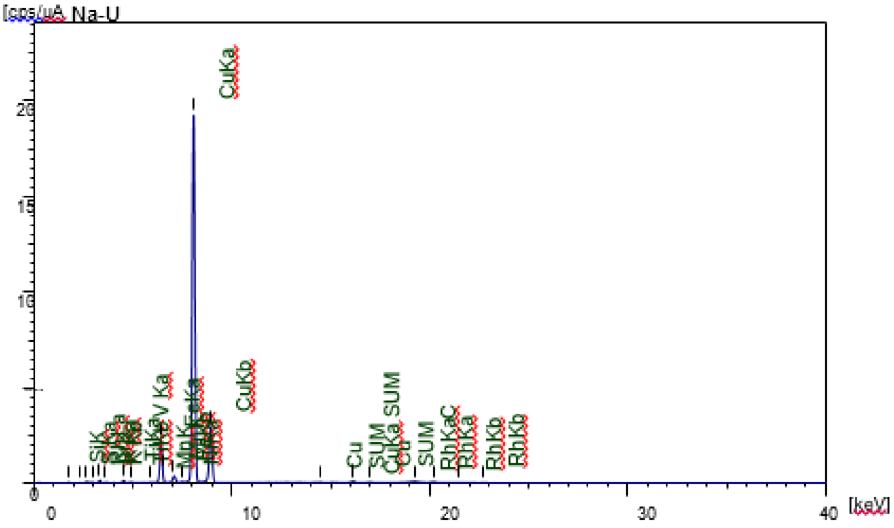

Fig. 14. EAV-HPU+Cu sample after the metal ions are added to the solution

3.4. Adsorption and desorption isotherms of EAV–HPG sorbent

Adsorption-desorption experiments of EAV-HPG sorbent were carried out in the Mak-Ben-Bakra device. Water vapor was used as adsorbate.

The samples prepared for the study were crushed to a powder state in an agate mortar, after mixing thoroughly, 1 g was taken out on a scale and placed in a cup. The pressure in the system was stabilized by vacuum for 6-8 hours.

Experiments conducted using water vapor at a temperature of 20°C in the Mak-Ben-Bakra device and calculations using the BET method revealed that the surface of the new substance obtained by organic modification of vermiculite with GIPAN and hexamine consists mainly of micropores and mesopores in Figure 15,16. The results of the calculation of the surface area and porosity of the sorbent are presented in Table 5.

3.5. Comparison results

As a result of this study, the sorbent obtained by the sorption of several metal ions was studied, and it was found to be selective for Cu (II) ion. About 100 scientific works on the process of obtaining composite sorbents like ours were studied. The existence of another composite obtained with the same composition as the obtained sorbent was not determined. Due to the complete porosity of the vermiculite, which forms the basis of the obtained sorbent, its density decreased. This helped the sorbent to have a small mass with a large volume Table 6.

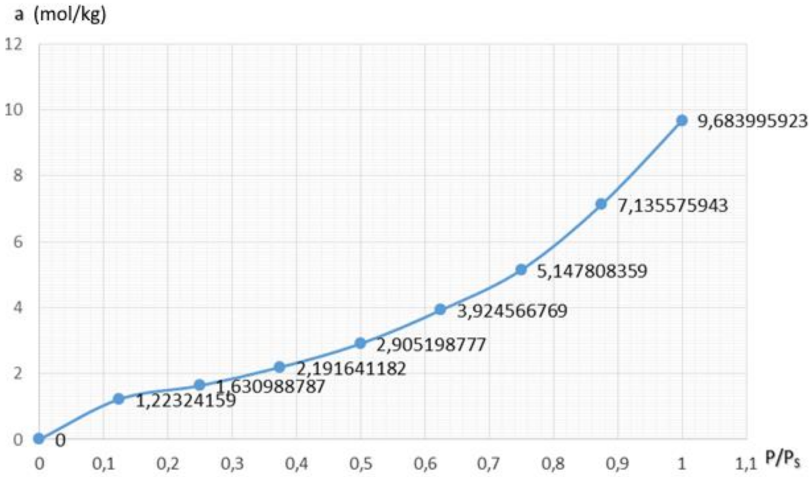

Fig. 15. Water vapor isotherm of EAV-HPU sorbent at 20 °C.

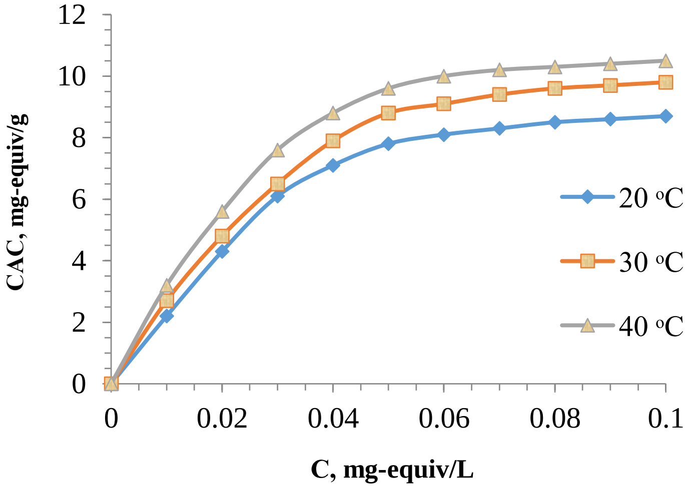

Fig. 16. Time dependence of metal sorption of VT/GI/U sorbent (S(Me)=0.05 N; sorb=30 mg, pH=4.2, V=10 ml).

Table 5. Calculation of the surface area of EAV-HPU sorbent.

A_m (monolayer capacity) mol/kg	S comparison, m^2/g	Micropore, W_0	Saturation Volume V_s	Mezogovak Wme	Pore radius
1.304	84.79	0.0913214	0.1744312	0.08	41.1Å 4.11nm

Table 6. The performance of the EAV-HPU sorbent compared to industrial sorbents is presented.

Sorbents	Functional group	Sorption capacity, mg-eq/l	Particle size, mm	Bulk density, g/l
VM/GP/U	NH; NH_2 -COOH; OH; COO	9.8	0.55-0.85	430
Purolite S950[1]	$–CH_2NHCH_2PO_3$	4.7	0.4-0.65	669
AFI-22[2]	$–N(CH_2CH_2OP{=}N–)_2OH$	3.6	0.63-1.0	405

[1] Purolite International Limited, England; [2] All-Russian Research Institute of Chemical Technology, Russia.

4. Conclusion

Hydrolyzed polyacrylonitrile and hexamine-modified vermiculite-based EAV-HPU composite sorbent without destroying the structure of the base-vermiculite with aluminosilicate layer, a highly effective sorbent was obtained as a result of increasing the active functional groups on the surface. DEC values helped to increase. A sharp increase in the amount of metal sorption from the solution confirmed the effectiveness of this method. It was found that the obtained sorbent is insoluble in water and has micro- and mesopores. Properties, physico-chemical properties, thermal tolerance, porosity level, SEM images of the surface of the obtained sample, elemental analysis, and the structure of existing bonds were studied using novel infrared spectroscopy methods.

Based on the BET method by absorbing water vapor at low pressure, the studied structural sorption properties of the sorbent showed that they have a microporous and mesoporous structure and high sorption properties.

Acknowledgements

The acknowledgment section helps identify the contributors responsible for specific parts of the research. It can include authors, non-authors, funding sources, editing services, or even administrative staff. It should only mention people directly involved with the research.

References

[1] G.A. Umirova, Kh.Kh. Turaev, B.K. Alimnazarov, Kasimov Sh.A., Jalilov A.T., Ibragimov B.T., Ashurov J.M., Crystal structure and Hirshfeld surface analysis of 8-azaniumylquinolinium tetrachloridozincate(II). *Crystallographica Section E: Crystallographic Communications*, 79 (2023) 856-860. https://doi.org/10.1107/S2056989023007466.

[2] Y. Baikin et al., Study of the natural mineral sorbents' absorption properties of the Ural region (Russia). *IOP Conference Series: Earth and Environmental Science*, 949 (2022). http://dx.doi.org/10.1088/1755-1315/949/1/012101.

[3] P. Piazzolla, Partial Stabilization of Cucumber Mosaic Virus (CMV) Induced by a Clay Mineral. *J. Phytopathol.*, 124 (1989). https://doi.org/10.1111/j.1439-0434.1989.tb04900.x.

[4] P. Kankan, K.M. Vinit, B. Santanu, S. Arijit, K.S. Ashok, et al., Role of Mg^{2+} and K^+ ions in retention of radio-cesium ($^{137}Cs^+$) in vermiculite clay. *J. Hazard. Mater. Adv.*, 13 (2024) 100411. http://dx.doi.org/10.1016/j.hazadv.2024.100411.

[5] H.M. Yang, K.S. Hwang, Ch.W. Park, K.W. Lee, Sodium-copper hexacyanoferrate-functionalized magnetic nanoclusters for the highly efficient magnetic removal of radioactive caesium from seawater. *Water Res.*, 125 (2017) 81–90. https://doi.org/10.1016/j.watres.2017.08.037.

[6] C. Latrille, O. Bildstein, Cs selectivity and adsorption reversibility on Ca-illite and Ca-vermiculite. *Chemosphere*, 288 (2022) 132582. https://doi.org/10.1016/j.chemosphere.2021.132582.

[7] N. Kanmaz, P. Demircivi, Construction of novel HKUST-1 supported vermiculite composite for excellent enhancement of malachite green adsorption. *Dye. Pigment.*, 226 (2024) 112153. https://doi.org/10.1016/j.dyepig.2024.112153.

[8] J.V. Veselovskaya et al., Novel ammonia sorbents "porous matrix modified by active salt" for adsorptive heat transformation: 3. Testing of "$BaCl_2$/vermiculite" composite in a lab-scale adsorption chiller. *Appl. Therm. Eng.*, 30 (2010) 1188–1192. https://doi.org/10.1016/j.applthermaleng.2009.11.001.

[9] I.K. Rind et al., Influential adsorption of Congo red using vermiculite/graphene/polyacrylamide composite. *Mater. Chem. Phys.*, 314 (2024) 128804. http://dx.doi.org/10.1016/j.matchemphys.2023.128804.

[10] A.D. Grekova, L.G. Gordeeva, Y.I. Aristov, Composite "LiCl/vermiculite" as advanced water sorbent for thermal energy storage. *Appl. Therm. Eng.*, 124 (2017) 1401–1408. https://doi.org/10.1016/j.applthermaleng.2017.06.122.

[11] Y.I. Aristov et al., A new methodology of studying the dynamics of water sorption/desorption under real operating conditions of adsorption heat pumps: Experiment. *Int. J. Heat Mass Transf.*, 51 (2008) 4966–4972. https://doi.org/10.1016/j.ijheatmasstransfer.2007.10.042.

[12] Y. Zhong et al., Isothermal sorption characteristics of the $BaCl_2$–NH_3 pair in a vermiculite host matrix. *Appl. Therm. Eng.*, 27 (2007) 2455–2462. https://doi.org/10.1016/j.applthermaleng.2007.02.011.

[13] F. Koksal, O. Gencel, M. Kaya, Combined effect of silica fume and expanded vermiculite on properties of lightweight mortars at ambient and elevated temperatures. *Constr. Build. Mater.*, 88 (2015) 175–187. https://doi.org/10.1016/j.conbuildmat.2015.04.021.

[14] S.V. Strelova et al., Composites "lithium chloride/vermiculite" for adsorption thermal batteries: Giant acceleration of sorption dynamics. *Energy*, 263 (2023) 125-133. https://doi.org/10.1016/j.energy.2022.125733.

[15] B. Balgysheva et al., Modified vermiculite of the mugodzhary deposit and its sorption properties. *J. Chem. Technol. Metall.*, 57 (2022) 533-546.

[16] V.E.D. Anjos et al., Montmorillonite and vermiculite as solid phases for the preconcentration of trace elements in natural waters: Adsorption and desorption studies of As, Ba, Cu, Cd, Co, Cr, Mn, Ni, Pb, Sr, V, and Zn. *Appl. Clay Sci.*, 99 (2014) 289–296. https://doi.org/10.1016/j.clay.2014.07.013.

[17] R. Fisher, Y. Ding, A. Sciacovelli, Hydration kinetics of K_2CO_3, $MgCl_2$ and vermiculite-based composites in view of low-temperature thermochemical energy storage. *J. Energy Storage*, 38 (2021) 102561. https://doi.org/10.1016/j.est.2021.102561.

[18] L.N.F. Queiroga, P.K. Soares, M.G. Fonseca, F.J.V.E. de Oliveira, Experimental design investigation for vermiculite modification: Intercalation reaction and application for dye removal. *Appl. Clay Sci.*, 126 (2016) 113–121. https://doi.org/10.1016/j.clay.2016.02.031.

[19] A.A. Ahatov, Kh.Kh. Turaev, A.Kh. Toshkulov, Synthesis, crystal structure and properties of tris(benzene-1.2-diamine-N,N′)-cadmium naphthalene-1,5-disulfonate trihydrate complex compound. *Indian Journal of Chemistry*, 63 (2024) 1036-1043. https://doi.org/10.56042/ijc.v63i10.12760.

[20] B.A. Muratov, Kh.Kh. Turaev, I.A. Umbarov, Sh.A. Kasimov, A.K. Nomozov, Studying of complexes of Zn(II) and Co(II) with acyclovir (2-amino-9-((2-hydroxyethoxy)methyl)-1,9-dihydro-6H-purine-6-OH). *Int. J. Eng. Trends Tech.*, 72 (2024) 202-208. https://doi.org/10.14445/22315381/IJETT-V72I1P120.

[21] Kh.Kh. Turaev, Kh.N. Eshankulov, I.A. Umbarov, Sh.A. Kasimov, A.K. Nomozov, D.A. Nabiev, Studying of

properties of bitumen modified based on secondary polymer wastes containing zinc. *Inter. J. Eng. Trends Tech.*, 71 (2023) 248-255. https://doi.org/10.14445/22315381/IJETT-V71I9P222.

[22] J. Gong et al., Organo-Vermiculites modified by aza-containing gemini surfactants: Efficient uptake of 2-naphthol and bromophenol blue. *Nanomaterials*, 12 (2022) 3636. https://doi.org/10.3390/nano122036364.

[23] L. Chauke et al., The removal of Rhodamine B from aqueous solution using manganese oxide modified vermiculite. *South African J. Chem. Eng.*, 47 (2024) 159–168. http://dx.doi.org/10.1016/j.sajce.2023.11.003.

[24] N.E. Fard, N.S. Ali, N.M.C. Saady, A review on development and modification strategies of MOFs Z-scheme heterojunction for photocatalytic wastewater treatment, water splitting, and DFT calculations. *Heliyon*, 10 (2024) p. 1-29. https://doi.org/10.1016/j.heliyon.2024.e32861.

[25] M. Gharagozlou, N.E. Fard, M. Ghahari, M.T. Yaraki, Bimetal Cu/Ni-BTC@SiO_2 metal-organic framework as high performance photocatalyst for degradation of azo dyes under visible light irradiation. *Environmental Research*, 256 (2024) 119229. https://doi.org/10.1016/j.envres.2024.119229.

[26] A.K. Nomozov, Kh.S. Beknazarov, S.Z. Khodjamkulov, Z.X. Misirov, S. Yuldashova, Synthesis of corrosion inhibitors based on (thio)urea, orthophosphoric acid and formaldehyde and their inhibition efficiency. *Baghdad Sci. J.*, 22 (2024) 19-27. https://doi.org/10.21123/bsj.2024.10590.

[27] S. Porgar, N. Rahmanian, Phase equilibrium for hydrate formation in the methane and ethane system and effect of inhibitors. *Chemical Review and Letters*, 5 (2022) 2-11. https://doi.org/10.22034/crl.2021.313255.1129.

[28] Sh.S. Nazirov, Kh.Kh. Turaev, Sh.A. Kasimov, B.A. Normurodov, Z.E. Jumaeva, A.K. Nomozov, Spectrophotometric determination of copper (II) ion with 7-bromo-2-nitroso-1-oxinaphthalene-3,6-disulphocid. *Indian J. Chem.*, 63 (2024) 500-505. https://doi.org/10.56042/ijc.v63i5.9289.

[29] M. Edraki, D. Zaarei, S. Hasan, The impact of green corrosion inhibitors on the protection performance of hybrid silane sol-gel coatings: A review. *Chemical Review and Letters*, 6 (2023) 428-441. https://doi.org/10.22034/crl.2023.425019.1259.

[30] M. Edraki, D. Zaarei, H.I. Sabeeh, The impact of green corrosion inhibitors on the protection performance of hybrid silane sol-gel coatings: A review. *Chemical Review and Letters*, 6 (2023) 428-441. https://doi.org/10.22034/crl.2023.425019.1259.

[31] N. Salehi, E. Vessally, L. Alkorta, I.M. Eshaghi, Nan@tetracyanoethylene (n=1-4) systems: Sodium salt vs sodium electride. *Chemical Review and Letters*, 3 (2020) 207-217. https://doi.org/10.22034/crl.2020.230543.1056.

[32] A.K. Nomozov, S.Ch. Eshkaraev, Z.E. Jumaeva, J.N. Todjiev, S.S. Eshkoraev, F.A. Umirqulova, Experimental and theoretical studies of Salsola oppositifolia extract as a novel eco-friendly corrosion inhibitor for carbon steel in 3% NaCl. *Inter. J. Eng. Trends Tech.*, 72 (2024) 312-320. https://doi.org/10.14445/22315381/IJETT-V72I9P126.

[33] R. Durdibaeva, K. Beknazarov, A. Nomozov, M. Demir, E. Berdimurodov, Exploring protective mechanisms with triazine ring and hydroxyethyl groups: Experimental and theoretical insights. *Kuwait J. Sci.*, 52 (2024) p. 100341. https://doi.org/10.1016/j.kjs.2024.100341.

[34] Kh.Kh. Turaev, Muqimov, Modern approach to the addition of organomineral additives to increase cement brand: A review. *Chemical Review and Letters*, 7 (2024) 804-815. https://doi.org/10.22034/crl.2024.467805.1381.

[35] Sh.S. Nazirov, Kh.Kh. Turaev, Sh.A. Kasimov, Kh.R. Tillaev, B.Sh. Alimnazarov, B.B. Abdullaeva, Spectrophotometric determination of Ni(II) ion with 7-bromo-2-nitroso-1-oxinaphthalene-3,6-disulphocid. *Int. J. Eng. Trends Tech.*, 72 (2024) 57-63.

[36] M.G. Yulchieva, Kh.Kh. Turaev, Sh.A. Kasimov, D.A. Nabiev, N.B. Chorieva, Research on the synthesis of nitrogen-containing sorbents. *Int. J. Eng. Trends Tech.*, 71 (2023) 161-167. https://doi.org/10.14445/22315381/IJETT-V71I8P214.

[37] S.A. Kholmurodova, Kh.Kh. Turaev, Preparation of vermiculite and polyacrylonitrile composite and its modification with diethanolamine. *Chemical Problems*, 1 (2025) 3-19. https://doi.org/10.32737/2221-8688-2025-1-3-19.

[38] M.J. Abduvalieva, Kh.Kh. Turaev, Sh.A. Kasimova, Complexing properties of ionite-polymer sorbent based on urea, formaldehyde and phenolsulfophthaleic acid. *Azerbaijan Chemical Journal*, 1 (2025) 127-138. https://doi.org/10.32737/0005-2531-2025-1-127-138.